Technical Paper

Transactions of the Society of
Naval Architects of Korea
Vol. 28, No. 1, April 1991
大韓造船學會論文集
第28卷 第1號 1991年 4月

A Numerical Simulation of Three-Dimensional Nonlinear Free Surface Flows

by

Chang-Gu Kang* and In-Young Gong*

3차원 비선형 자유표면 유동의 수치해석

강창구*, 공인영*

Abstract

In this paper, a semi−Lagrangian method is used to solve the nonlinear hydrodynamics of a three−dimensional body beneath the free surface in the time domain. The boundary value problem is solved by using the boundary integral method. The geometries of the body and the free surface are represented by the curved panels. The surfaces are discretized into the small surface elements using a bi−cubic B−spline algorithm. The boundary values of ϕ and $\frac{\partial \phi}{\partial n}$ are assumed to be bilinear on the subdivided surface. The singular part proportional to $\frac{1}{R}$ are subtracted off and are integrated analytically in the calculation of the induced potential by singularities.

The far field flow away from the body is represented by a dipole at the origin of the coordinate system. The Runge−Kutta 4−th order algorithm is employed in the time stepping scheme. The three−dimensional form of the integral equation and the boundary conditions for the time derivative of the potential is derived. By using these formulas, the free surface shape and the equations of motion are calculated simultaneously. The free surface shape and the forces acting on a body oscillating sinusoidally with large amplitude are calculated and compared with published results. Nonlinear effects on a body near the free surface are investigated.

요 약

자유표면하에서 움직이는 임의의 형상의 3차원 물체로 인한 비선형 유체력을 준 Lagrangian 방법을 사용하여 해석하였다. 경계치 문제는 경계 적분 방법(Boundary Integral Method)을 이용하여 해결하였으며, 물체와 자유 표면의 형상은 곡면 Panel로 표현하였다. 이들 표면은 bi−cubic B−spline 방법을 사용하여 유한개의 작은 표면 요소로 나뉘어지게 되며, 또한 ϕ와 $\frac{\partial \phi}{\partial n}$ 은 표면 요소상

Manuscript received : October 12, 1990, revised manuscript received : December 28, 1990.

*Member, Korea Research Institute of Ship and Ocean Engineering

에서 bi-linear하다고 가정한다. 특이점에 의한 유기 포텐시얼의 계산시 1/R에 비례하는 부분은 제거하고 해석적으로 처리하였다.

물체로부터 멀리 떨어진 곳에서의 유체 유동은 좌표계의 원점에 위치한 Dipole로 표현하였으며, Time Stepping시 Runge-Kutta의 4차 방법을 사용하였다. 3차원인 경우에 대한 적분 방정식과 포텐시얼의 시간 미분값에 대한 경계 조건이 유도되었으며, 이러한 식들을 사용하여 자유표면의 형상과 물체의 운동을 동시에 계산하였다. 대진폭을 가지고 규칙적으로 진동하는 물체에 작용하는 힘과 이때의 자유 표면 형상을 계산하고 기 발표된 자료와 비교하여 보았으며, 자유표면 근처에서 운동하는 물체에 작용하는 비선형 효과를 관찰하였다.

1. Introduction

In the design of submerged bodies operating near free surface the free surface effects are considered. The linearized theories for the free surface problem were developed during many decades. Recently the nonlinear free surface problem is solved in the time domain by the semi-Lagrangian methodl

Longuet-Higgins and Cokelet[1] presented a mixed Eulerian-Lagrangian method for following the time history of space-periodic irrotaional surface waves. The only independent variables at the beginning of each time step were the coordinates and velocity potential of marked particles on the free surface. At each time-step an integral equation was solved for the new normal component of velocity. This method was applied to a free, steady wave of finite amplitude, and was found to give excellent agreement with calculations based on Stoke's series. It was then extended to unsteady waves, produced by initially applying an asymmetric distribution of pressure to a symmetic, progressive wave. The results showed the freely running wave then steepened and overturned.

Using a technique similar to that of Longuet-Higgins and Cokelet[1], Faltinsen[2] solved a nonlinear two dimensional free surface problem including a harmonically oscillating body. The body intersected the free surface and was constrained to move in the vertical direction. The numerical calculations were reduced by representing the flow far away from body as a dipole located at the center of the body. A formula to calculate the exact force on the body was presented. It was only necessary to know the velocity protential on the positions of the free surface and the wetted body surface.

A numerical method for the time simulation of the nonlinear motions of two dimensional surface piercing bodies of arbitrary shapes in water of finite depth was presented by Vinje & Brevig[3]. Periodicity in space was assumed. At each time step, Cauchy's integral theorem was applied to calculate the complex potential and its time derivative along the boundary. The solution was stepped forward in time by integrating the exact kinematic and dynamic free-surface boundary conditions as well as the equation of motion for the body. They solved the problem of capsizing in beam seas, caused by extreme waves.

Two-dimensional nonlinear free surface problems by a dipole (vortex and source) distribution method were solved by Baker, et al. [4]. The resulting Fredholm integral equation of the second kind was solved by iteration which reduced storage and computing time. Applications to breaking water waves over finite-bottom topography and interacting triads of surface and interfacial waves were given.

The semi-Lagrangian method was extended to vertically axisymmetric free surface flows by

Dommermuth & Yue[5]. Since they sloved the finite depth problem, a far field closure was implemented by matching the linearized soultion outside a radiation boundary. The intersection line between the body and free surface was treated by extending Lin's[6] method.

The nonlinear hydrodynamics of an axisymmetric body beneath the free surface in the time domain were solved by Kang & Troesch[7]. The free surface shape and the forces acting on a sphere osciilating sinusoidally with large amplitude are calculated and compared with published results. The far field flow away from the body is represented by a dipole at the origin of the coordinate system similar to Faltinsen[2]. This is only valid until waves arrive. Waves generated by the numerical error at the truncation boundary are not observed.

In this paper, the method used for axisymmetric flows by Kang and Troesh[7] is extended to three-dimensional free surface flows. The free surface shape and the forces acting on a three-dimensional body oscillating sinusoidally with large amplitude are calculated and compared with published results. When the body motion is unknown, the time derivative of the potential on the body is needed for the time simulation. In two dimensions, Vinje & Brevig [8] derived the integral equation and the boundary conditions for the time derivative of the potential and stream function. However their formulas may not be extended to three-dimensional problems. The three-dimensional form is derived in this work. By using these formula, the free surface shape and the equations of motion are calculated simultaneously. The Runge-Kutta 4-th order algorithm is employed in the time stepping scheme(See Appendix 1).

Numerical calculations are performed for the following cases :

(a) A body oscillating vertically near the free surface

(b) A body oscillating horizontally near the free surface.

2. Mathematical Formulation

Consider an ideal fluid below the surface given by $F(\underline{x}, t)=0$, where $\underline{x}(x, y, z)$ is a right-handed coordinate system with z positive upwards and the origin located at the mean free surface. The fluid is assumed to be inviscid and incompressible and the flow is assumed to be irrotational. The fluid domain is bounded with the following surfaces, the free surface, S_F, the body, S_B, and the surfaces at infinity, S_∞(Fig.1). The surfaces, taken as a whole, will be denoted as S. The governing equation and the boundary conditions are as follows(Longuet-Higgins & Cokelet[1] and Dommermuth & Yue[5]) :

Laplace equation :

$$\nabla^2\phi=0 \quad \text{in the fluid domain} \tag{1}$$

Kinematic free surface condition :

$$\frac{D\underline{x}}{Dt}=\nabla\phi \quad \text{on} \quad F(\underline{x}, t)=0 \tag{2}$$

Dynamic free surface condition

$$\frac{D\phi}{Dt}=-gz+\frac{1}{2}\nabla\phi\cdot\nabla\phi \quad \text{on} \quad F(\underline{x}, t)=0 \tag{3}$$

Body boundary condition :

$$\nabla\phi\cdot\underline{n}(\underline{x}, t)=\underline{V}\cdot\underline{n} \quad \text{on} \quad B(\underline{x}, t)=0 \tag{4}$$

Radiation condition :

$$\phi\to 0 \text{ as } |\underline{x}|\to\infty, \ t<\infty \tag{5}$$

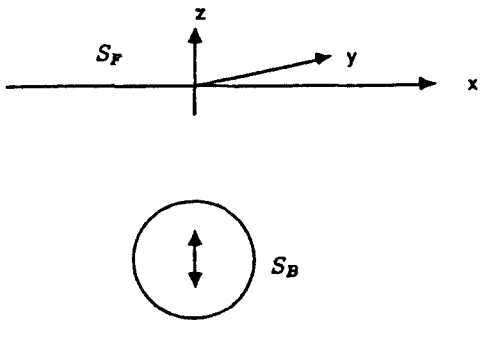

Fig. 1 Coordinate System

where $\frac{D}{Dt}=(\frac{\partial}{\partial t}+\nabla\phi\cdot\nabla)$ is the substantial derivative, $F(\underline{x}, t)=0$ is the function representing the free surface geometry at time t, $\underline{V}$ includes both translational and rotational velocities, and $B(\underline{x}, t)=0$ is the function representing the body surface geometry at time t. As an initial condition, ϕ is zero everywhere at $t=0$.

The Green function, $G(\underline{x};\underline{y})$, satisfies the following equation.

$$\nabla^2 G(\underline{x};\underline{y})=-\delta(\underline{x}-\underline{y}) \quad (6)$$

where $\underline{x}$ is the vector to the field point, $\underline{y}$ is the vector to the source point, and $\delta(\underline{x}-\underline{y})$ is the Dirac delta function. Through the application of Green's second identity in the fluid domain, the potential is given as

$$\alpha(\underline{x}, t)\phi(\underline{x}, t)=\iint_S[\frac{\partial\phi}{\partial n}-\phi\frac{\partial}{\partial n}]GdS \quad (7)$$

where α is an included solid angle at $\underline{x}$. In this problem, α is 2π on the surface.

The Green function that satisfies Eq. (6) is

$$G(\underline{x}, \underline{y})=\frac{1}{R}=\frac{1}{|\underline{x}-\underline{y}|} \quad (8)$$

where $\underline{x}$ is the position vector of a field point and $\underline{y}$ is that of a source point.

The solution of Eq. (3) gives the potential ϕ on the free surface $F(\underline{x}, t)=0$. Also ϕ_n on the body is known from the body boundary condition, Eq.(4). The normal and tangential velocities on the free surface are needed to solve Eq.(3). The normal velocity on the free surface is a solution of Eq.(7). Details to calculate the tangential velocity is given in the section 3. Consequently, a Fredholm integral equation of the second kind on the body and of the first kind at the free surface may be solved.

2.1 Far Field Condition

The far field condition is important in the nonlinear free surface problem. It can be resolved by using periodic boundary conditions if the physical problem has spatial periodicity(Longuet-Higgins & Cokelet, [1]). Faltinsen[2] and Kang[9] assumed that the behavior of the potential is like that of a dipole at the origin of the coordinate system.

A far field closure by matching the nonlinear computational solution to a general linear solution of transient outgoing radiated waves was used by Dommermuth & Yue[5]. This method is mathematically complete.

A numerical radiation condition was posed so as no waves reflected from the truncated surface(Yang & Liu[10]). They found that the usual one-dimensional Sommer-feld condition gave reasonable results for an axisymmetric cylinder heaving in the still water. Also it was extended to 2-D case for the cylinder swaying in the still water.

In this work. the far field closure simiar to that used by Faltinsen[2] and Kang[9] is posed. It is simple and it works well until waves arrive at the truncation boundary.

At the far field, the velocity potential, ϕ, and the wave elevation, η, are small from the radiation condition, Eq.(5). For example,

$$\phi(z=\eta)=\phi(z=0)+\eta\frac{\partial\phi}{\partial z}(z=0)+\text{H.O.T.} \quad (9)$$

Assuming the behavior of the potential, ϕ, is like that of a dipole at the origin of the coordinate system, it follows that as $r\to\infty$

$$\begin{aligned}&\phi=(z=0)=0\\&\frac{\partial\phi}{\partial z}(z=0)\sim\frac{1}{r^3}\\&\eta=\int_0^t\frac{\partial\phi}{\partial z}(z=0)dt\sim\int_0^t\frac{1}{r^3}dt\\&\phi(z=\eta)\sim\eta\frac{\partial\phi}{\partial z}(z=0)\sim\frac{1}{r^6}\end{aligned} \quad (10)$$

where r is $\sqrt{x^2+y^2}$. This is only valid until waves arrive at the truncation boundary.

If we take a large value of r, the potential ϕ on the free surface must be relatively small to

the vertical velocity $\frac{\partial \phi}{\partial z}$. Therefore the effect of the potential at the far field can be neglected. The far field condition is approximately satisfied by including the effect of the vertical velocity $\frac{\partial \phi}{\partial z}$ at the far field.

3. Numerical Implementation

The body surface and the free surface are discretized into the small surface elements ΔS_{ij} using a bicubic B−spline algorithm(Barsky & Greenberg[11]). The surfaces $\Delta S_{ij}(x, y, z)$ can be represented by the parameters, u and v. Thus

$$x_{ij}(u, v) = \sum_{s=-2}^{1} \sum_{t=-2}^{1} b_s(u)\, V^x_{i+s,\, j+t} b_t(v)$$

$$y_{ij}(u, v) = \sum_{s=-2}^{1} \sum_{t=-2}^{1} b_s(u)\, V^y_{i+s,\, j+t} b_t(v) \qquad (11)$$

$$z_{ij}(u, v) = \sum_{s=-2}^{1} \sum_{t=-2}^{1} b_s(u)\, V^z_{i+s,\, j+t} b_t(v)$$

for $0 \le u \le 1$ and $0 \le u \le 1$

where $b_s(u)$ and $b_t(u)$ are the uniform cubic B−spline basis functions and V_{ij} are vertices (See Appendix 2). This allows the curved panels.

The end condition should be imposed to get a complete B−spline approximation. There are several methods to impose end conditions according to the geometrical characteristics(Barsky[12]). The derivative of B−spline interpolation at the end is set to get the tangent of the given geometry if the tangent is known. If the tangent is not known, the derivative at the end is set to be the slope between two vertices at the end obtained by using B−spline algorithm.

The boundary values of ϕ and $\frac{\partial \phi}{\partial n}$ are assumed to be bilinear on the subdivided surface ΔS_{ij} as shown below.

$$\phi = a_0 + a_1 u + a_2 v + a_3 uv$$

$$\frac{\partial \phi}{\partial n} = b_0 + b_1 u + b_2 u + b_3 uv \qquad (12)$$

for $0 \le u \le 1$ and $0 \le v \le 1$

To evaluate the integrals over the segments the two point Gaussian Quadrature formula (Ferziger[13], Abramowitz & Stegun[14]) is used when the field point is not a corner of the pannel. In Eq. (7). G_n is not singualr but G has $(\frac{1}{R})$ type singularity in the transformed $u-v$ domain as the field point approaches the source point. The singularity is integrable and can be integrated by numerical quadrature. But since an accurate integration of the singularity requires a higher order quadrature formula, the method following Ferziger[13] and Dommermuth & Yue[5] can be used. The integral can be factored into the sum of the $(\frac{1}{R})$ type singular part which is integrable analytically and the non−singular part which requires numerical quadrature(Ferziger[13]).

3. 1 Removel of $(\frac{1}{R})$ type singularity

In Eq.(7), G has $(\frac{1}{R})$ type singularity as the field point approaches the source point. The $(\frac{1}{R})$ type singularity is integrable in the surface integration.

$$I = \iint_{\Delta S_{ij}} \phi_n \frac{1}{R} dS \qquad (13)$$

First, consider the induced potential at (f_{00}, g_{00}, h_{00}), which is one of the corners of panel, by the source panel ΔS_{ij}. Eq. (11) can alternatively be represented by the following equations:

$$x' = \sum_{i=0}^{3} \sum_{j=0}^{3} f_{ij} u^i v^j$$

$$y' = \sum_{i=0}^{3}\sum_{j=0}^{3} g_{ij}u^i v^j \qquad (14)$$

$$z' = \sum_{i=0}^{3}\sum_{j=0}^{3} h_{ij}u^i v^j$$

By using Eqs.(14) and (40), dS and R can be transformed and expanded into Taylor's series about $u=0$, $v=0$ as follows:

$$\begin{aligned} dS &= |J|\,dudv \\ &= \sqrt{EG-F^2}\,dudv \\ &= \{[(\frac{\partial x'}{\partial u})^2+(\frac{\partial y'}{\partial u})^2+(\frac{\partial z'}{\partial u})^2]\times[(\frac{\partial x'}{\partial v})^2 \\ &\quad +(\frac{\partial y'}{\partial v})^2+(\frac{\partial z'}{\partial v})^2]-(\frac{\partial x'}{\partial u}\frac{\partial x'}{\partial v}+\frac{\partial y'}{\partial u}\frac{\partial y'}{\partial v} \\ &\quad +\frac{\partial z'}{\partial u}\frac{\partial z'}{\partial v})^2\}^{1/2}dudv=[J_0+H.O.T.]dudv \end{aligned} \qquad (15)$$

where

$$\begin{aligned} J_0 &= \{(f_{10}g_{01}-f_{01}g_{10})^2+(g_{10}h_{01}-g_{01}h_{10})^2 \\ &\quad +(h_{10}f_{01}-h_{01}f_{10})^2\}^{1/2} \end{aligned} \qquad (16)$$

and

$$\begin{aligned} R &= \{(x-x')^2+(y-y')^2+(z-z')^2\}^{1/2} \\ &= \{(-f_{10}u-f_{01}v\cdots)^2+(-g_{10}u-g_{01}v\cdots)^2 \\ &\quad +(-h_{10}u-h_{01}v\cdots)^2\}^{1/2} \\ &= \sqrt{Au^2+Buv+Cv^2}+H.O.T. \end{aligned} \qquad (17)$$

where

$$\begin{aligned} A &= f_{10}^2+g_{10}^2+h_{10}^2 \\ B &= 2(f_{10}f_{01}+g_{10}g_{01}+h_{10}h_{01}) \\ C &= f_{01}^2+g_{01}^2+h_{01}^2 \end{aligned} \qquad (18)$$

The integral, I, can be divided into two parts. One of them includes singular part in the integrand and the other does not include singular part. After some manipulations of Eq. (13) by using Eqs. (14)~(18), the first integral I_1 becomes

$$I_1 = b_0J_0\int_0^1\int_0^1 \frac{dudv}{(Au^2+Buv+Cv^2)^{1/2}} \qquad (19)$$

The integral, I_1, can be evaluated in closed form as follows(Gradsteyn & Ryzhik[15], Forbes[16]):

$$\begin{aligned} I_1 = b_0J_0\Big[&\frac{1}{\sqrt{A}}\ln(2A+B+2\sqrt{A(A+B+C)}) \\ &-\frac{1}{\sqrt{A}}\ln(B-2\sqrt{AC}) \\ &+\frac{1}{\sqrt{C}}\ln(2C+B+2\sqrt{C(A+B+C)}) \\ &-\frac{1}{\sqrt{C}}\ln(B+2\sqrt{AC})\Big] \end{aligned} \qquad (20)$$

The second one can be described as follows:

$$I_2 = \int_0^1\int_0^1\Big[\frac{(b_0+b_1u+b_2v+b_3uv)J}{R} - \frac{b_0J_0}{\sqrt{Au^2+Buv+Cv^2}}\Big]dudv \qquad (21)$$

The integrand of the integral, I_2, does not have $(\frac{1}{R})$ type sigularity near $u=0$ and $v=0$. Thus I_2 can be obtained accurately even by the two point Gaussian Quadratur. Similarly, the integral (13) can be obtained at the rest corners $(u=0, v=1)$, $(u=1, v=0)$, and $(u=1, v=1)$.

To get the tangential velocity, the velocity potential ϕ on the surfaces can be represented by the bicubic B-spline (See Appendix 2). Even if this representation is inconsistent with Eq. (12), it gives smooth variation of the tangential velocity on the surface.

The derivatives ϕ_u and ϕ_v are obtained by differentiating the potential with respective to u and v respectively. Generally, the tangential vector $\underline{t}_v(f_u, g_u, h_u)$ along u-axis is not perpendicular to the vector $\underline{t}_v(f_v, g_v, h_v)$ along v-axis. Therefore Gram-Schmidt orthogonalization is needed to get the orthogonal tangential vector on the surface.

4. Calculation of the Time Derivative of Potential

For the time simulation, $\frac{\partial\phi}{\partial t}$ should be known to calculate the forces and moments acting on the body. In two dimensions Vinje & Brevig [8] derived an integral equation and boundary

condition for $\frac{\partial\phi}{\partial t}$ by using the ϕ and Ψ formulation. However, their results can not be extended to the three-dimensional case. Since $\frac{\partial}{\partial n}(\frac{\partial\phi}{\partial t})$ can not be calculated by using the given motion, a boundary value problem for $\frac{\delta\phi}{dt}$, the time derivative of the potential in body fixed coordinates, is derived as follows :

$$\begin{aligned}&\frac{\delta}{dt}(\frac{\partial\phi}{\partial n})\\&=\underline{n}\cdot\frac{\delta}{dt}\nabla\phi+\nabla\phi\cdot\frac{\delta\underline{n}}{dt}\\&=\underline{n}\cdot[\frac{\partial}{dt}\nabla\phi+(\underline{V}\cdot\nabla)\nabla\phi]+\nabla\phi\cdot(\underline{\omega}\times\underline{n})\\&=\underline{n}\cdot[\nabla\frac{\partial\phi}{dt}+\nabla(\underline{V}\cdot\nabla\phi]+\underline{\omega}\times\nabla\phi]+\nabla\phi\\&\quad\cdot(\underline{\omega}\times\underline{n})\\&=\frac{\partial}{\partial n}(\frac{\delta\phi}{dt})\end{aligned}\tag{22}$$

which can be expressed as

$$\frac{\partial}{\partial n}(\frac{\delta\phi}{dt})=\underline{n}\cdot(\frac{\partial\underline{V}_T}{\partial t}+\dot{\underline{\omega}}\times\underline{r}-\underline{\omega}\times\underline{V}_T)\tag{23}$$

Following the nomenclature of Vinje & Brevig[8], the operator $\frac{\delta}{dt}$ is $(\frac{\partial}{\partial t}+\underline{V}\cdot\nabla)$, $\underline{V}=\underline{V}_T+\underline{\omega}\times\underline{r}$, $\underline{V}_T$ is the translational velocity of the center of mass of the body, $\underline{r}$ is the position vector to the boundary from the center of mass of the body, and $\underline{\omega}$ is the angular velocity vector of the body. Eq.(23) is useful in that most quantities of interest are expressed in the body coordinate system rather than a fixed, inertial one.

Since $\underline{V}\cdot\nabla\phi$ satisfies Laplace equation, the time derivative of the potential, $\frac{\delta\phi}{dt}$, can be calculated by using Green's theorem. The limiting behavior of $\underline{V}\cdot\nabla\phi$ at $r\to\infty$ can also be checked, or

$$\underline{V}\cdot\nabla\phi=O(r\frac{\phi}{r})=O(\phi)\quad\text{as}\quad r\to\infty\tag{24}$$

Applying Green's theorem for $\frac{\delta\phi}{dt}$ instead of ϕ in Eqs. (1), (6), and (7), the following equation can be obtained :

$$\alpha\frac{\delta\phi}{dt}=\iint_S[\frac{\partial}{\partial n}(\frac{\delta\phi}{dt})-(\frac{\delta\phi}{dt})\frac{\partial}{\partial n}]GdS\tag{25}$$

R.H.S. of Eq. (23) may be represented as follows:

$$\underline{n}\cdot\left(\frac{\partial\underline{V}_T}{\partial t}+\dot{\underline{\omega}}\times\underline{r}-\underline{\omega}\times\underline{V}_T\right)=\sum_{i=1}^{6}a_in_i\tag{26}$$

where $\underline{n}=(n_1,\ n_2,\ n_3)$ and $\underline{r}\times\underline{n}=(n_4,\ n_5,\ n_6)$.

The time derivative of the potential, $\frac{\delta\phi}{dt}$, can be decomposed as follows:

$$\frac{\delta\phi}{dt}=\sum_{i=1}^{6}a_i\frac{\delta\phi_i}{dt}+\frac{\delta\phi_7}{dt}\tag{27}$$

The auxiliary terms, $\frac{\delta\phi_i}{dt}$ and $\frac{\delta\phi_7}{dt}$, are solutions of the following boundary value problems:

$$\frac{\partial}{\partial n}(\frac{\delta\phi_i}{dt})=n_i\quad\text{and}\quad\frac{\partial}{\partial n}(\frac{\delta\phi_7}{dt})=0\quad\text{on } B(\underline{x},\ t)=0\tag{28}$$

and

$$\frac{\delta\phi_i}{dt}=0\text{ and }\frac{\delta\phi_7}{dt}=\underline{V}\cdot\nabla\phi-\frac{1}{2}\nabla\phi\cdot\nabla\phi-gz\quad\text{on}\quad F(\underline{x},\ t)=0\tag{29}$$

The time derivative of the potential on the free surface, $\frac{\delta\phi_7}{dt}$, is calculated by using solutions of the integral equation. Eq.(7).

5. The Pressures and Forces

Once the time derivative of the potential is known, the pressures are found by applying Bernoulli's equation. Bernoulli's Equation is derived for the variables relative to an inertial coordinate system. However, it is convenient for the purpose of solving the boundary value pro-

blem to use body fixed coordinates. Under these circumstances, spatial differentiation is invariant with coordinate transformation, but temporal differentiation is not. Bernoulli's equation can be expressed as

$$\frac{p}{\rho} = -\frac{\partial\phi}{\partial t} - \frac{1}{2}\nabla\phi\cdot\nabla\phi - gz$$

$$= -\frac{\delta\phi}{dt} + \underline{V}\cdot\nabla\phi - \frac{1}{2}\nabla\phi\cdot\nabla\phi - gz. \quad (30)$$

The term $\frac{\delta\phi}{dt}$ in the above equation is calculated by Eq.(27). With the pressure known, the force and moment become

$$\underline{F} = m\dot{\underline{V}}$$

$$= \iint_S p\underline{n}dS - mg\underline{k}$$

$$= -\rho\iint_S \underline{n}\left(\frac{\delta\phi}{dt} - \underline{V}\cdot\nabla\phi + \frac{1}{2}\nabla\phi\cdot\nabla\phi + gz\right)$$

$$dS - mg\underline{k} \quad (31)$$

$$\underline{M} = \iint_S p\underline{r}\times\underline{n}dS.$$

For three−dimensional bodies the force and moment are rearranged as follows:

$$\underline{F} = \underline{F}_1 + \underline{F}_2 + (\rho g\nabla - mg)\underline{k} \quad (32)$$

$$\underline{M} = \underline{M}_1 + \underline{M}_2$$

where ∇ in Eq. (32) is the displaced volume of the body,

$$\underline{F}_1 = -\rho\iint_{S_B}\underline{n}\frac{\delta\phi}{dt}\,dS,$$

$$\underline{F}_2 = -\rho\iint_{S_B}\underline{n}\left(\underline{V}\cdot\nabla\phi - \frac{1}{2}\nabla\phi\cdot\nabla\phi\right)dS, \quad (33)$$

$$\underline{M}_1 = -\rho\iint_{S_B}\underline{r}\times\underline{n}\frac{\delta\phi}{dt}\,dS, \text{ and}$$

$$\underline{M}_2 = -\rho\iint_{S_B}\underline{r}\times\underline{n}\left(\underline{V}\cdot\nabla\phi - \frac{1}{2}\nabla\phi\cdot\nabla\phi\right)dS.$$

6. Numerical Calculation

6. 1 Heave motion

To demonstrate the usefulness of the technique shown in the previous section, the force acting on a sphere oscillating beneath the free surface is determined. The motion of a sphere is given by $z = -h + a\cos\omega t$ for t greater than zero. Initially the potential and wave elevation at the free surface are zero.

The number of elements on the body is 200 and that on the free surface is 40×40. The truncation boundary is the position from the origin of the cordinate system where waves reaches in four periods of the body motion ($-16\le x/R\le 16$, $-16\le y/R\le 16$). So, it depends on the group velocity of wave. Even spacing is used on the body and free surface. The typical time interval is approximately 0.05 period of motion for the time simulation of the sphere.

The mean depth of immersion for the center of the sphere, h, is h/R=2.0. The time history of the force acting on the oscillating sphere with a large ratio of motion amplitude, a, to radius, R, (a/R=0.5) was calculated and is compared with the results of the axisymmetric free surface problem (Kang & Troesch[7]) in Fig. 2. They show good agreement. In the reference [7], the calculation results for the sphere oscil-

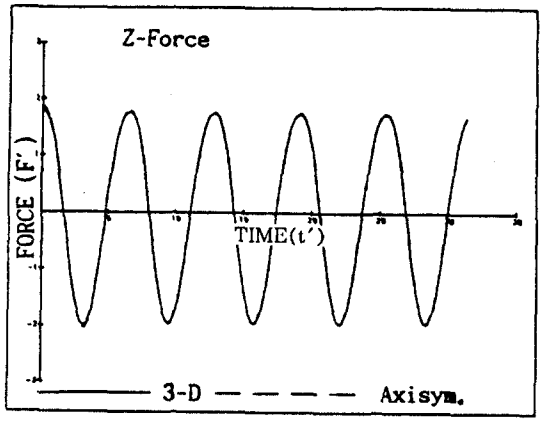

Fig. 2 Comparison of Heave Force Acting on the Sphere by 3−D and Axisymmetric Solutions (a/R=0.5, h/R=2.0, KR=1.0)

lating vertically with small amplitude showed good agreement with those given by Ferrant [17]. This means the 3−D algorithm in this paper works well.

In Fig.3, the time history of force components which consist of F_1 and F_2 is shown. The forces are nondimensionalized by $\rho g K a R^3$, where K is a wave number, ω^2/g, and g is the gravitational constant and the time t is nondimensionalized by $\sqrt{R/g}$. The harmonic distributions of the total force are shown in Table 1. The second order amplitude of the force is 6.5% of the first

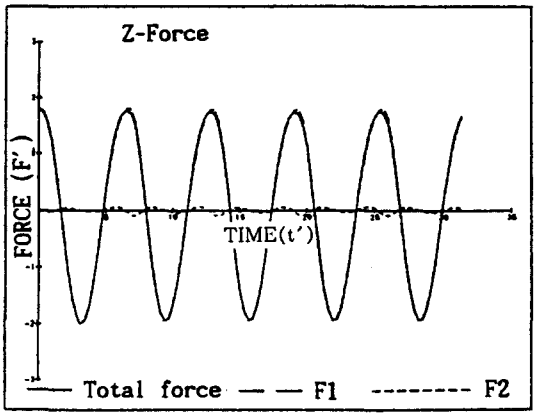

Fig. 3 Time History of the Heave Force Components Acting on the Heaving Sphere (a/R=0.5, h/R=2.0, KR=1.0)

Table 1 Harmonic Distributions of the Total Force for Heave Motion (a/R=0.5, h/R=2.0, KR=1.0)

Heave Force	$F/\rho g K a R^3$	
I−TH	COS	SIN
0	−0.2850707E−01	0.0000000E+00
1	0.1843049E+01	0.2665849E+00
2	−0.1033978E+00	0.6141333E−01
3	0.6449880E−01	0.8355246E−02
4	−0.5114811E−02	−0.1019468E−01
5	0.2418429E−01	0.2957444E−02

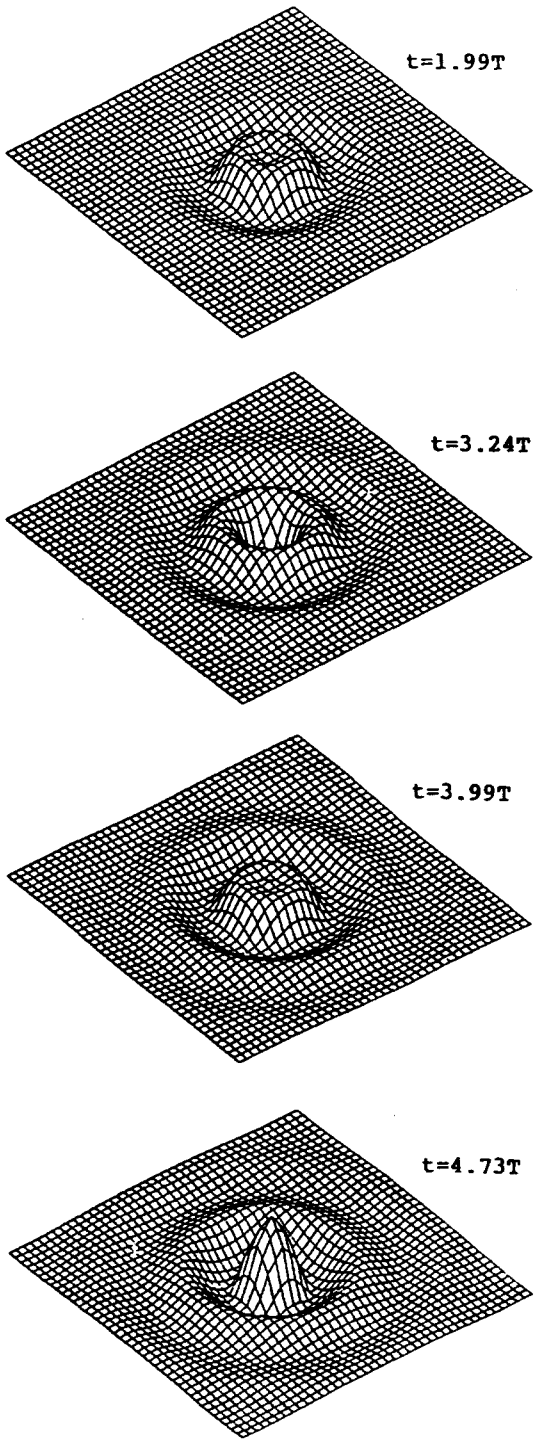

Fig. 4 Wave Profiles for Heave Motion (a/R=0.5, h/R=2.0, KR=1.0)

order one. And the mean force is 1.5% of the first order. Fig. 4 shows the three dimensional wave profiles at four different times. All the wave profiles are exaggerated by factor of 50 in z-direction. In the figures T is a period of the motion.

6. 2 Surge motion

The surge motion of the sphere is given by $x=a\cos\omega t$ for t greater than zero. The mean depth of immersion for the center of the sphere is $h/R=2.0$. The amplitudes of the motion is $a/R=0.5$. The nondimensionalized wave number, KR, is equal to 1.0.

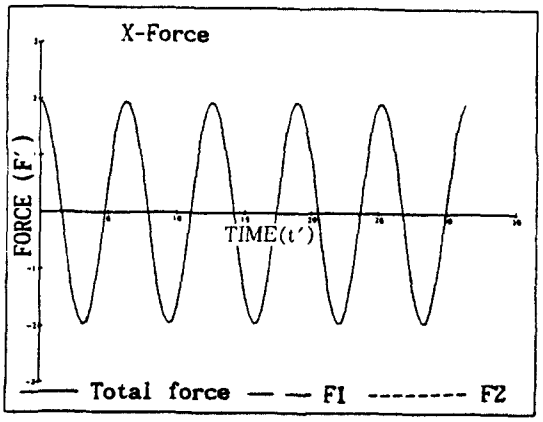

Fig. 5 Time History of the Surge Force Components Acting on the Surging Sphere (a/R=0.5, h/R=2.0, KR=1.0)

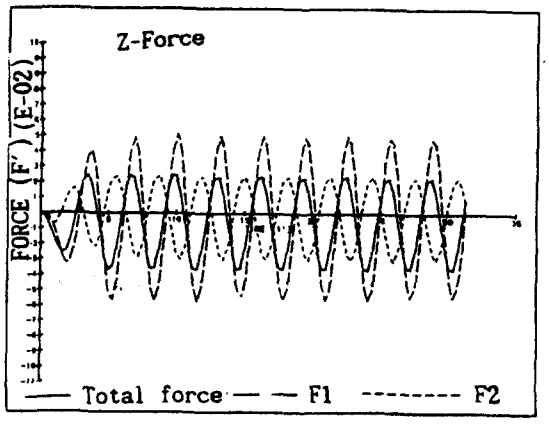

Fig. 6 Time History of the Heave Force Components Acting on the Surging Sphere (a/R=0.5, h/R=2.0, KR=1.0)

The time histories of the forces acting on the sphere are shown in Fig. 5-6. The harmonic distributions of the horizontal and vertical forces are given in Table 2. The three dimensional wave profiles at 4 different times are shown in Fig. 7.

In case of surge motion, the first order surge force is dominant unlike the heave motion. However nonlinear effects appear only in the vertical force. The first order vertical force is negligible, but the mean and second order vertical forces are not. The mean vertical force is important for a submerged body to keep a constant depth.

Table 2 Harmonic Distributions of the Total Force for Surge Motion (a/R=0.5, h/R=2.0, KR=1.0)

Surge Force $F/\rho gKaR^3$

I-TH	COS	SIN
0	-0.1308621E-02	0.0000000E+00
1	0.1927655E+01	0.1237885E+00
2	0.2138726E-03	-0.1002954E-02
3	0.3005543E-01	0.1583521E-02
4	-0.1381397E-04	-0.4408678E-03
5	0.2590462E-01	-0.4266882E-03

Heave Force $F/\rho gKaR^3$

I-TH	COS	SIN
0	-0.1274143E-01	0.0000000E+00
1	-0.4001656E-03	0.4211906E-04
2	0.2037149E-01	0.2325045E-01
3	-0.3133378E-03	0.8355940E-04
4	-0.3846344E-03	-0.2575103E-03
5	-0.2204935E-03	0.9557988E-04

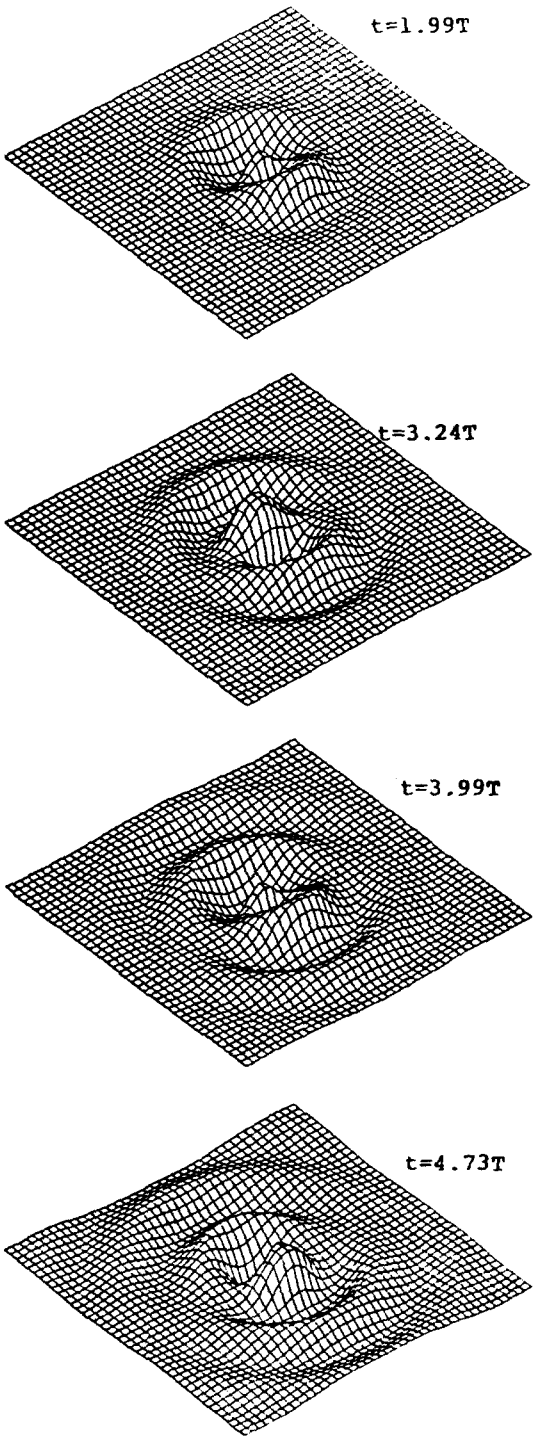

Fig. 7 Wave Profiles for Surge Motion (a/R=0.5, h/R=2.0, KR=1.0)

6.3 Advancing motion

Saw-tooth instability is not observed in the computation of the oscillatory motions. But it seems to be inevitable and break down the numerical time stepping in case of advancing sphere. It may be due to short waves generated by the body. The length of short waves is less than the mesh size in this computation. The numerical error does not die out but was accumulated continuously. Eventually the numerical scheme breaks down. Thus a simple numerical filtering scheme are tried to avoid break down, but still does not work well. Fig. 8 shows the wave profile before breakdown.

All the calculations were carried out on CRAY2S and each solution time was approximately 50,000 seconds.

7. Conclusion

The nonlinear hydrodynamics of a three-dimensional body beneath the free surface is solved in the time domain. The free surface shape and forces acting on a sphere advancing and oscillating sinusoidally with large amplitude are calculated and compared with published re-

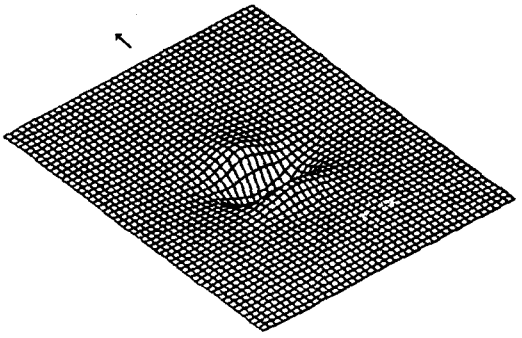

Fig. 8 Wave Profile Generated by an Advancing Sphere($U = 2.557 m/sec$ for $2.557 < t$, $U = t$ for $0 < t < 2.557$, $h/R = 2.0$, $t = 3.6 sec$)

sults. The far filed flow away from the body is represented by a three dimensional dipole at the origin of the coordinate system. This is only valid until waves arrive at the truncation boundary. Any numerical instability was not observed in the computation of the oscillatory motions. But a simple numerical filtering scheme was used to avoid breakdown in computation of advancing body. The integral equation and boundary conditions to calculate the time derivative of the potential on the body are derived. By using these formulas, the free surface shape and forces are calculated simultaneously. A Runge−Kutta 4th order scheme is employed in the solution method. Nonlinear effects on the oscillating body submerged in infinite water depth are studied.

Acknowledgment

This work was supported by the Basic Research Program, contract ED 469 of the Korea Research Institute of Ships and Ocean Engineering (KRISO). Acknowledgement is also given to the Ministry of Science and Technology of Korea (MOST). The authors should appreciate Dr. Choung Mook Lee for his encouragements.

References

[1] Longuet−Higgins, M.S. & Cokelet, E.D., "The Deformation of Steep Surface Waves on Water, I. A Numerical Method of Computation," Proc. R. Soc. Lond. A., 350, pp. 1−26, 1976

[2] Faltinsen, O.M., "Numerical Solution of Transient Nonlinear Free−Surface Motion Outside or Inside Moving Bodies," Proc. 2nd Intl. Conf. on Num. Ship Hydro., U.C. Berkeley, 1977.

[3] Vinje, T. & Brevig, P., "Nonlinear Ship Motions," Proc. 3rd Intl. Conf. on Numerical Ship Hydrodynamics, Paris, 1981.

[4] Baker, G.R., Meiron, D.I. & Orsag, S.A., "Generalized Vortex Methods for Free−surface Flow Problems," Journal of Fluid Mechanics, 123, pp. 477−501, 1982.

[5] Dommermuth, D.G. & Yue, D.K.P., "Study of Nonlinear Axisymmetric Body−Wave Interactions," In Proc. 16th Symp. on Naval Hydrodynamics, Berkely, 1986.

[6] Lin, W.M., "Nonlinear Motion of the Free Surface near a Moving Body," Ph.D. Thesis, M.I.T., Dept. of Ocean Engineering, 1984.

[7] Kang, C.−G.& Troesch, A.W., "Nonlinear Interation betwwen Axisymmetric Bodies and The Free Surface−Body in Water of Infinite Depth," Proc. the Seminar on Ship Hydrodynamics to honor Prof. J.H.Hwang, Seoul, Korea, 1988.

[8] Vinje, T. & Brevig, P., "Nonlinear, Two Dimensional Ship Motions," Seminar on the Norweigan Ships in Rough Seas(SIS) Project, 1982.

[9] Kang, C.−G., "Bow Flare Slamming and Nonlinear Free Surface−Body Interaction in the Time Domain," Ph.D. Thesis, Univ. of Michigan, 1988.

[10] Yang, C. & Liu, Y.Z., "Time−Domain Calculation of the Nonlinear Hydrodynamics of Wave−Body Interaction," 5th Intl. Conf. on Num. Ship Hydro., Hiroshima, 1989.

[11] Barsky, B.A. & Greenberg, D.P., "Determining a Set of B−Spline Control Vertices to Generate an Interpolating Surface," Computer Graphics and Image Process 14, pp. 203−226, 1980.

[12] Barsky, B.A., "End Conditions and Boundary Conditions for Uniform B−Spline Curve and Surface Representations," Computers in Industry 3, pp. 17−29, 1982.

[13] Ferziger, J.H., Numerical Methods for Engineering Application, John Wiley and

Sons, Inc., 1981.

[14] Abramowitz, M. & Stegun, I. A., Handbook of Mathematical Functions, Government Printing Office, Washington, 1964.

[15] Gradsteyn, I.S. and Ryzhik, I.M., Table of Integrals, Series, and Products, Academic Press, 1980.

[16] Forbes, L.K., "An Algorithm for 3-Dimensional Free-Surface Problems in Hydrodynamics," Journal of Computational Physics 82, pp. 330-347, 1989.

[17] Ferrant, P., "Sphere immergee en mouvement de pilonnement de grande amplitude," Premiers Journes De L'hydrodynamique, Nantes, 1987.

[18] Kaplan, W., Advanced Mathematics for Engineers, Addison-Wesley Publishing Co.

Appendix 1. The 4th order Runge-Kutta method [13]

When $y' = f(x, y)$ is nonlinear, this can be solved by Runge-Kutta methods. The most commonly used Runge-Kutta methods are fourth order accurate and there are a number of these. The best known such method (sometimes called the fourth order Runge-Kutta method) is

$$y^{*}_{n+1/2} = y_n + \frac{h}{2} f(x_n, y_n)$$

(Euler predictor-half step)

$$y^{**}_{n+1/2} = y_n + \frac{h}{2} f(x_{n+1/2}, y^{*}_{n+1/2})$$

(Backward Euler corrector-half step)

$$y^{***}_{n+1} = y_n + hf(x_{n+1/2}, y^{**}_{n+1/2}) \qquad (34)$$

(Midpoint rule predictor-full step)

$$y_{n+1} = y_n + \frac{h}{6}[f(x_n, y_n) + 2f(x_{n+1/2}, y^{*}_{n+1/2}) + 2f(x_{n+1/2}, y^{**}_{n+1/2}) + f(x_{n+1}, y^{***}_{n+1})]$$

(Simpson's rule corrector-full step)

Looking at this method one can see that derivation of such methods is not easy task. An analysis of it for the general case is also difficult. It is not too difficult to analyze, however, when applied to $y' = \alpha y$. We find that

$$y_{n+1} = (1 + \alpha h + \frac{(\alpha h)^2}{2} + \frac{(\alpha h)^3}{6} + \frac{(\alpha h)^4}{24}) y_n \qquad (35)$$

so that method is indeed fourth order accurate and the error is of order $(\alpha h)^5/120$. It is interesting to note that the steps that comprise this method are of order one, one, two, and four, repectively, and the method has inherited the accuracy of the final corrector.

Appendix 2. Parametric Uniform B-spline Surface Representation [11]

A B-spline surface is defined in a piecewise manner, where each piece is a segment of the surface called a surface patch. The entire surface is a mosaic of these patches sewn together with appropriate continuity (Fig. 9). A bicubic B-spline surface consists of patches which are cubic in each of the two parametric directions and it is everywhere continuous along with its first and second derivative vectors, in both directions. This continuity constraint reduces to requiring continuity of the first and second parametric derivative vectors across the borders of

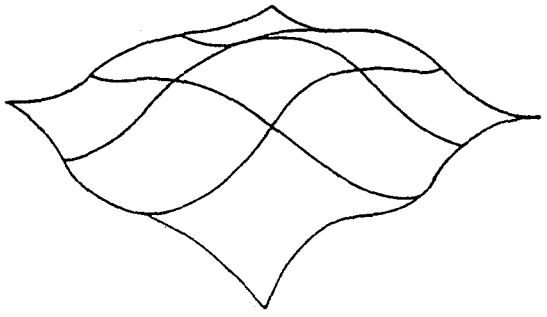

Fig. 9 A B-Spline Surface is a Mosaic of Surface Patches.

adjacent patches. The B−spline surface is defined by, but does not interpolate, a set of points called control vertices. These control vertices form a two−dimensional array, Although the vertices actually exist in three−dimensional x−y−z space, they are organized as a two−dimensional graph. Each vertex is either an interior vertex or a boundary vertex. This notion can be formalized quite elegantly by drawing on graph theory. The set of control vertices can be considered as a graph V, E whose vertices form the set

$$V=\{\, V_{ij} \mid i=0, \cdots, m\,;\, j=0, \cdots, n\}$$

and with the set of edges

$$E=\{(V_{ij},\ V_{i,j+1}) \mid i=0, \cdots, m-1\,;\, j=0, \cdots, n\}$$
$$\cup\{(V_{ij},\ V_{i+1,j}) \mid i=0, \cdots, m-1\,;\, j=0, \cdots, n\}$$

The interior vertices are the vertices V_{ij}, where $1 \le i \le m-1$ and $1 \le j \le n-1$, and the boundary vertices are V_{0j}, $j=0, \cdots, n-1$, V_{in}, $i=0, \cdots, m-1$, V_{mj}, $j=1, \cdots, n$, and V_{i0}, $i=1, \cdots, m$. To emphasize this graph−theoretic interpretation, the term control graph to describe the set of control vertices is chosen (Fig. 10). A major advantage of the B−spline formulation is that it is a local representation. A bicubic B−spline surface patch is controlled by 16 control vertices and is unaffected by all other control vertices.

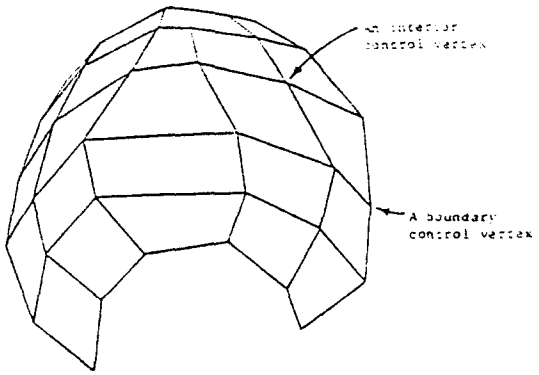

Fig. 10 A B−Spline Control Graph

Conversely, a given control vertex exerts influence over only 16 surface patches and has no effect on the remaining patches. This means that the effects of moving a control vertex are limited to 16 patches. A point on the (i, j)th uniform bicubic B−spline surface patch is a weighted average of the 16 vertices $V_{i+r,\ j+s}$, $r=-2, -1, 0, 1$ and $s=-2, -1, 0, 1$. The mathematical formulation for the patch Q_{ij} (u, v) is then

$$Q_{ij}(u, v)=\sum_{r=-2}^{1}\sum_{s=-2}^{1} bb_{rs}(u, v)\, V_{i+r,\ j+s}$$
$$for\ 0 \le u, v \le 1 \qquad (36)$$

The set of bivariate uniform basis functions is the tensor product of the set of univariate uniform basis functions. That is,

$$bb_{rs}(u, v)=b_r(u)b_s(v)$$
$$for\ r=-2, -1, 0, 1,\ and$$
$$s=-2, -1, 0, 1 \qquad (37)$$

Thus, the formulation for the patch $Q_{ij}(u, v)$ can be rewritten as

$$Q_{ij}(u, v)=\sum_{r=-2}^{1}\sum_{s=-2}^{1} b_r(u)\, V_{i+r,\ j+s}b_s(v)$$
$$for\ 0 \le u, v \le 1 \qquad (38)$$

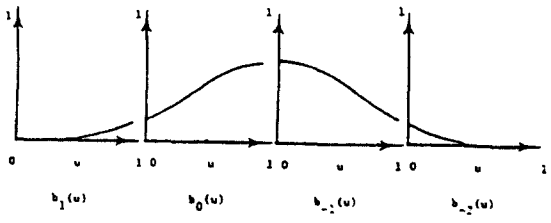

Fig. 11 Graphs of the Univariate Uniform Cubic B−Spline Basis Functions

The univariate uniform cubic B−spline basis functions are graphed in Fig. 11, and can be written in matrix form as

$$[b_{-2}(u)\ b_{-1}(u)\ b_0(u)\ b_1(u)] = [u^3 u^2 u^1]1/6 \begin{bmatrix} -1 & 3 & -3 & 1 \\ 3 & -6 & 3 & 0 \\ -3 & 0 & 3 & 0 \\ 1 & 4 & 1 & 0 \end{bmatrix} \quad (39)$$

Appendix 3 Calculation of the Surface Integral and the Normal Vector

The surface integral can be calculated as follows (Kaplan, [18]) :

$$\iint_S H(x, y, z)\, d\sigma = \iint_{Suv} H[f(u, v), g(u, v), h(u, v)] \sqrt{EG-F^2}\, du\, dv \quad (40)$$

where

$x = f(u, v),\ y = g(u, v),\ z = h(u, v)$

$\underline{P}_1 = x_u\underline{i} + y_u\underline{j} + z_u\underline{k}$

$\underline{P}_2 = x_v\underline{i} + y_v\underline{j} + z_v\underline{k}$

$$E = |\underline{P}_1|^2 = \left(\frac{\partial x}{\partial u}\right)^2 + \left(\frac{\partial y}{\partial u}\right)^2 + \left(\frac{\partial z}{\partial u}\right)^2$$

$$F = \underline{P}_1 \cdot \underline{P}_2 = \frac{\partial x}{\partial u}\frac{\partial x}{\partial v} + \frac{\partial y}{\partial u}\frac{\partial y}{\partial v} + \frac{\partial z}{\partial u}\frac{\partial z}{\partial v}$$

$$G = |\underline{P}_2|^2 = \left(\frac{\partial x}{\partial v}\right)^2 + \left(\frac{\partial y}{\partial v}\right)^2 + \left(\frac{\partial z}{\partial v}\right)^2$$

The normal vector on the surface S is calculated by using the following formula.

$$\underline{n} = \frac{\underline{P}_1 \times \underline{P}_2}{|\underline{P}_1 \times \underline{P}_2|} \quad (41)$$